

## Research Article

# SOL-GEL SYNTHESIS AND CHARACTERIZATION OF ZINC SUBSTITUTED NICKEL FERRITE MAGNETIC NANOPARTICLES

\*Priyadharshini, M., Dr. Jesurani, S., Ranjani, M. and Vennila, S.

Department of Physics, Jayaraj Annapackiyam College for women (autonomous) Periyakulam 625601

### ARTICLE INFO

#### Article History:

Received 15<sup>th</sup> March 2016

Received in revised form

24<sup>th</sup> April 2016

Accepted 19<sup>th</sup> May 2016

Published online 30<sup>th</sup> June 2016

#### Keywords:

Sol-gel, Ferrites,  
Nanoparticles, X-ray diffraction.

### ABSTRACT

Zinc substituted Nickel ferrite ( $\text{Ni}_{1-x}\text{Zn}_x\text{Fe}_2\text{O}_4$  with  $x=0.0, 0.1, 0.2, 0.3, 0.4$ , and  $0.5$ ) magnetic nanoparticles were synthesized using sol-gel method. Nickel nitrate, ferric nitrate, zinc nitrate were used as raw materials. The samples were characterized by TG-DTA, FTIR, XRD and VSM. The functional group analyzed by FT-IR. The XRD used to analyze phase structure and lattice parameters. The powder calcined at 800 °C XRD patterns confirmed the formation of Nickel ferrite single phase. The crystallite sizes of Zinc substituted Nickel ferrite particles were calculated using Debye-Scherer's relation. The crystallite size decreases 25 nm to 55 nm, with increasing the concentration of zinc. TG/DTA measurement showed the weight loss between 0-200°C, 200-400°C and 400-600°C which corresponding the endothermic and exothermic processes. An exothermic peak observed at around 400°C is due to the thermal decomposition of the ingredients to form  $\text{NiFe}_2\text{O}_4$ . The saturation magnetization value is 0.2 emu/g to 0.7 emu/g for the sample sintered at 800°C.

Copyright©2016, Priyadharshini et al. This is an open access article distributed under the Creative Commons Attribution License, which permits unrestricted use, distribution, and reproduction in any medium, provided the original work is properly cited.

## INTRODUCTION

Magnetic properties of Ni-Zn- $\text{Fe}_2\text{O}_4$  have attracted attention because of their use at high frequency applications. Because of high resistivity and Zinc doped  $\text{NiFe}_2\text{O}_4$ , (Cullity, 1972) and magnetic properties for technical application hence it is widely used in capacitor (Patil Basavani and Rathod sopan, 2014) and magnetic cores of read-write heads for high speed digital recording and production of electronic and magnetic components (Meskin et al., 2006). Which are depends on various parameters such as processing conditions. Researchers are used a variety of techniques including alternative sputtering technology, Pulse-Laser deposition (Rezlescu et al., 2000) and spin-spray plating etc to deposit film However most of them cannot be economically applied on a large scale because they required high vacuum system (Awati, 2015). Complicated experimental steps and high reaction temperatures Ni-Zn ferrite is very limited (Hsu et al., 2015). The sol-gel method was used for synthesis of this Nano ferrites material (Ashwani Sharma, 2013).  $\text{NiFe}_2\text{O}_4$  has inverse spinal structure with  $\text{Ni}^{2+}$ ions in octahedral sites and  $\text{Fe}^{3+}$  ions equally distributed (Visinescu et al., 2010) between tetrahedral and octahedral sites whereas  $\text{ZnFe}_2\text{O}_4$  has a normal spinal structure with  $\text{Zn}^{2+}$ ions in tetrahedral and  $\text{Fe}^{3+}$  in octahedral sites (Xie et al., 2004). Therefore, Zn substitution in  $\text{NiFe}_2\text{O}_4$  may have some distorted spinal structures depending upon the concentration of the precursor solutions (Mariyan Sharifi Jebeli, 2013).

\*Corresponding author: Priyadharshini, M.,

Department of Physics, Jayaraj Annapackiyam College for women (autonomous) Periyakulam 625601.

## Experimental procedure

### Preparation

The samples were synthesized using nickel nitrate, zinc nitrate, and iron nitrate. All the chemicals were supplied by Modern scientific chemicals Ltd. Ethylene glycol, oxalic acid as a gelling agent because it plays an important role in homogeneous mixing. Nickel nitrate dissolve in ethanol, Zinc nitrate dissolve in ethanol, and ferric nitrate dissolve in ethanol then Zinc nitrate slowly added with Nickel nitrate, next Nickel nitrate added with ferric nitrate, and then oxalic acid dissolve in 2ml of ethanol, finally drop wise ethylene glycol added while stirring at 90°C, after the solutions was evaporated with continuously stirred to obtain uniform gel. After 1-2 hours the gel is formed. The brownish powder obtained is subjected to calcinations at 800° C for 3hrs.

## RESULTS AND DISCUSSION

### TG-DTA analysis

The thermal decomposition of  $\text{NiFe}_2\text{O}_4$  nanoparticles is shown in Figure (2). The TGA curve of Nickel ferrite shows three main steps of mass loss. The first stage of degradation can be observed between 0 and 200°C, with respect to the output of waste water which is adsorbed on the material during the synthesis step. The corresponding DTA curve indicates that these processes are exothermic at temperature 200 and 400°C.

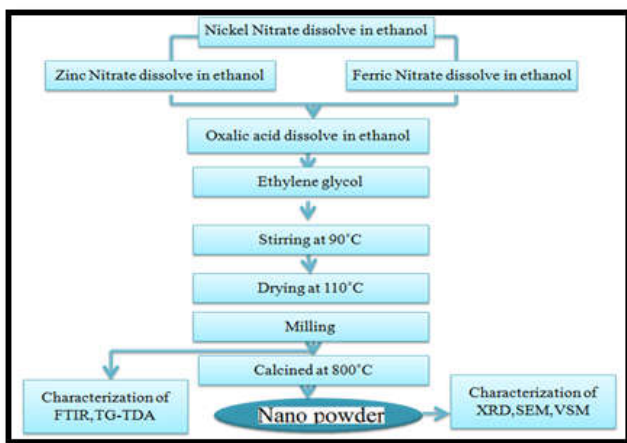


**Fig. 1.** Synthesis of nickel ferrite nano powder

The second stage of degradation occurs between 200-400°C, Loss in weight results due to evaporation of moisture or solvent. The third step weight loss occurs in the temperature range of 400-600°C with the removal of organic impurities still remaining in the material after 800°C. A continuous line in the TGA curve is related to the end of the degradation of ions and oxalic acid.

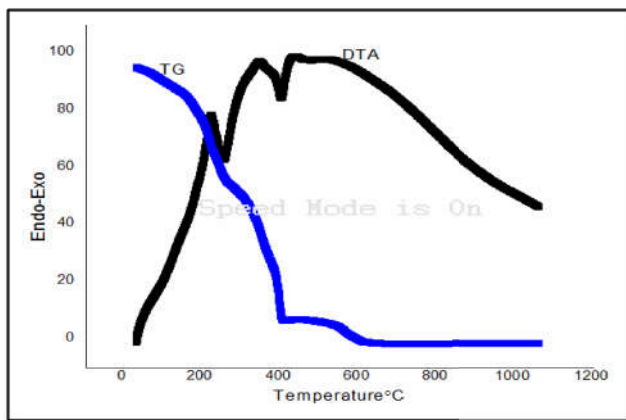


**Fig. 2.** DTA and TG plots of the dried gels for  $\text{Ni}_{1-x}\text{Zn}_x\text{Fe}_2\text{O}_4$

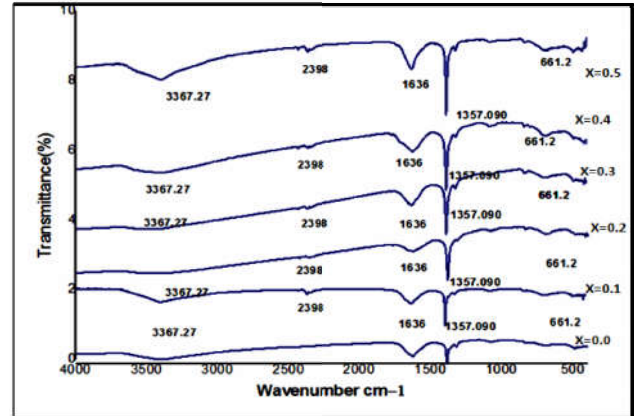
#### FT-IR analysis

Figure (3) shows the FTIR spectrum of the  $\text{Ni}_x\text{Fe}_2\text{O}_4$  nanoparticles synthesized by sol gel method, which was acquired in the range of 400-4000  $\text{cm}^{-1}$ . The peaks are at 2398  $\text{cm}^{-1}$  and 3367  $\text{cm}^{-1}$  corresponding to the stretching vibration of  $\text{C}\equiv\text{N}, \text{N}-\text{H}$  respectively as shown in the fig (3). Nickel ferrite IR curve fig (3) shows the absorptions of ferrite with a strong absorption around 1357  $\text{cm}^{-1}$  to the intrinsic vibrations of the nitro compounds groups with respect to the N-O symmetric stretch bond. There are two weak and broad absorption peaks at around 1500 and 1600  $\text{cm}^{-1}$  corresponding to the presence of small amounts of residual carbon in the samples. Then 661  $\text{cm}^{-1}$  is the C-Br stretching represented by alkyl halides groups.

#### Structural analysis

Figure (4) shows the X-ray diffraction (XRD) patterns of typical samples of  $\text{Ni}_{1-x}\text{Zn}_x\text{Fe}_2\text{O}_4$  [Where  $x=0.0, 0.1, 0.2, 0.3, 0.4, 0.5$ ]. The major planes correspond to (531), (220), (311), (400), (422), (511) were found to be matched which confirmed the presence of cubic nanoparticles.

In the XRD pattern of nickel ferrite nanoparticles diffraction peaks at 35°, 42°, 55°, 57° and 63° can be assigned to cubic spinel structure. The X-ray diffraction patterns show well developed diffraction lines assigned to cubic single phase, with all major peaks matching with the standard pattern of Ni-Zn ferrite, JCPDS 08-0234. The broadening of the Bragg's peaks indicates the formation of nickel.



**Fig.3.** FTIR spectra of  $\text{Ni}_{1-x}\text{Zn}_x\text{Fe}_2\text{O}_4$  with  $(x=0.0, 0.1, 0.2, 0.3, 0.4, \text{ and } 0.5)$

The average crystallite sizes decreases from 25-55nm using Scherrer's formula.

$$D = k \lambda / (\beta \cos \theta)$$

In which, where  $k$  is a constant taken as 0.9,  $\theta$  is the diffraction angle;  $\lambda$  is the wavelength of the X-ray radiation.  $\beta$  is the full width half maximum (FWHM) of each phase and  $D$ =average particle size of crystallite.

$$a = d_{hkl}/(h^2+k^2+l^2)^{1/2}$$

Where  $(hkl)$  are the miller indices and  $d_{hkl}$  is interplanar spacing. The X-ray density ( $\rho_{\text{X-ray}}$ ) was calculated from the relation,

$$\rho_{\text{X-ray}} = 8M/\text{Na}^3$$

Where,  $M$  is the molecular weight,  $N$  the Avogadro number and "a" is the lattice constant. The calculated values of crystallite size, lattice constant,  $d$  spacing, and X-ray densities are tabulated in Table (1).

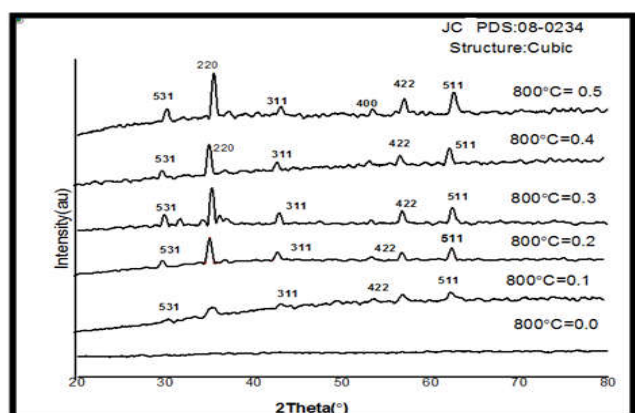


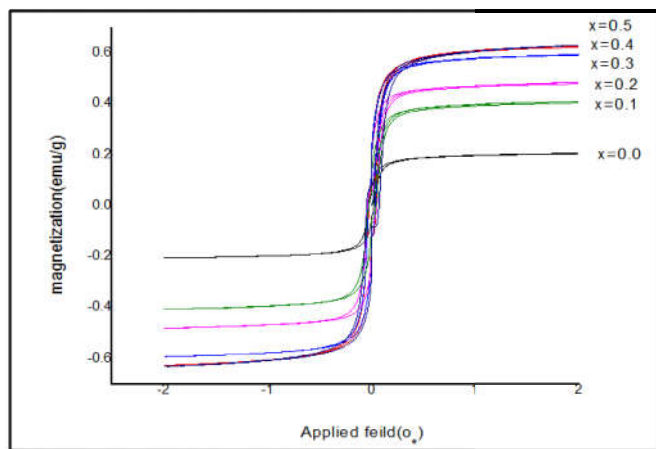
**Fig. 4.** XRD patterns of  $\text{Ni}_{1-x}\text{Zn}_x\text{Fe}_2\text{O}_4$  with  $(x=0.0, 0.1, 0.2, 0.3, 0.4 \text{ and } 0.5)$

**Table 1. Variation of crystallite size, lattice constant, d-spacing, and X-ray density with nickel ferrite concentration**

Ni Fe <sub>2</sub> O <sub>4</sub> Concentration	Crystallite size (nm)	Lattice constant (Å)	d spacing (Å)	X-ray density (g/cm <sup>3</sup> )
X=0.0	55.38	8.3429	2.1430	3.7325
X=0.1	43.50	8.3558	2.0640	3.7263
X=0.2	37.72	8.3731	2.1151	3.7186
X=0.3	31.20	8.3864	2.2619	3.7128
X=0.4	29.97	8.4213	2.1374	3.6973
X=0.5	25.24	8.4456	2.1468	3.6867

### Magnetic measurements

The magnetic properties were studied from the VSM graph shown in the Figure (5). Temperature values of saturation magnetization (Ms). The increase of saturation magnetization with increasing Zn concentration. The particles are soft magnetic material at 800°C. All the samples show narrow hysteresis loop which indicates the soft ferrite nature. Hysteresis loops of synthesized sample are shown in fig (5) saturation magnetization value is 0.2 emu/g to 0.7emu/g for the sample sintered at 800°C.

**Fig. 5. hysteresis loops of Ni<sub>1-x</sub>Zn<sub>x</sub>Fe<sub>2</sub>O<sub>4</sub> sintered at 800°C**

### Conclusions

Zn substituted NiFe<sub>2</sub>O<sub>4</sub> nanoparticles can be prepared by the sol-gel method. From FTIR patterns analyzed the functional group. The formation of cubic phase Nickel ferrite was confirmed by the XRD technique. The synthesis of nanoparticles with crystalline size and lattice constant decreases from 25-55nm for 800°C.

From VSM studies, the effect of Zinc substitution on saturation magnetization was analyzed. It showed that there is an increase in saturation magnetization for all the concentration of Nickel ions and were explained using Neel's two sub lattice model. The 800°C N-H hysteresis curve show that particles are soft magnetic at 800°C.

### REFERENCES

- Ashwani Sharma, I., Mahabir Singh and Satya Prakash Sharma, Sanjay Kumar, 2013. Simple synthesis and magnetic properties of nickel-zinc ferrites nanoparticles by using Aloe vera extract solution, 5 (6):145-151.
- Awati, V.V. 2015. Synthesis and characterization of Ni-Cu-Zn Ferrite materials by auto-combustion Technique,page no:50-57.
- Cullity, B.D. 1972. Introduction to Magnetic Materials, Addison Wesley Publishing Co. Inc., Reading.
- MA.Chikazumi, Physics of Magnetism, Wiley, New York, page no 195.
- Hsu, J. Y., Ko, W. S., Chen, C. J. 2015. The effect of V2O5 on the sintering of Ni-Cu-Zn ferrite page no: 67-82.
- Mariyan Sharifi Jebeli, Norani Muti Binti 2013. Mohamad synthesis and characterization of Ni-Zn ferrite based nanoparticles by sol-gel technique page no: 45-53.
- Meskin, P. E., V. K. Ivanov, A. E. Barantchikov, B. R. Churagulov and Y. D. Tretyakov, 2006. "Ultrasonically Assisted Hydrothermal Synthesis of Nanocrystalline ZrO<sub>2</sub>TiO<sub>2</sub>, NiFe<sub>2</sub>O<sub>4</sub> and Ni<sub>0.5</sub>Zn<sub>0.5</sub>Fe<sub>2</sub>O<sub>4</sub> Powders," Ultrasonics Sono chemistry, Vol. 13, No. 1, pp. 47-53.
- Patil Basavani and Rathod sopan, M Synthesis and characterization and magnetic properties of Co<sup>2+</sup> substituted Ni nanoferrite by sol-gel Auto- cumbustion Method page no: 13404 (2014).
- Rezlescu, E., Sachelarie, L., Popa, P. D., Rezlescu, N. 2000. Effect of substitution of divalent ions on the electrical and magnetic properties of Ni-Zn-Me ferrites. IEEE Trans Magn; 3962–3967.
- Visinescu, D., C. Paraschiv, A. Lanculescu, B. Jurca, B. Vasila and O. Carp, Dyes and Pigments 87, 125-131 (2010).
- Xie, X., X. Zhang, B. Yu, H. Gao, H. Zhang, W. Fei, 2004. "Rapid extraction of genomic DNA from saliva for HLA typing on microarray based on magnetic nanobeads", Magnetism and Magnetic Materials, vol. 280, No.2-3, pp.164–168.

\*\*\*\*\*